pollutants

MDPI

Article

Transfer of 7 Organic UV Filters from Sediment to the Ragworm *Hediste diversicolor*: Bioaccumulation of Benzophenone-3 and Further Proof of Octocrylene Metabolism

Fanny Clergeaud, Sonja K. Fagervold, Alice M. S. Rodrigues, Evane Thorel, Didier Stien and Philippe Lebaron *

Laboratoire de Biodiversité et Biotechnologies Microbiennes, CNRS, Sorbonne Université, USR3579, Observatoire Océanologique, 66650 Banyuls-sur-Mer, France; clergeaud@obs-banyuls.fr (F.C.); fagervold@obs-banyuls.fr (S.K.F.); alice.rodrigues@obs-banyuls.fr (A.M.S.R.); thorel@obs-banyuls.fr (E.T.); didier.stien@cnrs.fr (D.S.)

* Correspondence: lebaron@obs-banyuls.fr

Abstract: Organic UV filters are continuously released in aquatic ecosystems due to their widespread use, especially in touristic coastal environments. Generally, organic UV filters are poorly soluble in water and tend to accumulate in the sediment compartment. This represents a conceivable risk for sediment-dwelling organisms and a potential for transfer of the UV filters up the food chain. This study aimed to assess the potential transfer of seven UV filters including benzophenone-3 (BP3), bis-ethylhexyloxyphenol methoxyphenyl triazine (BEMT), butyl methoxydibenzoylmethane (BM), methylene bis-benzotriazolyl tetramethylbutylphenol (MBBT), 2-ethylhexyl salicylate (ES), diethylhexyl butamido triazone (DBT), and octocrylene (OC) from artificial spiked sediment (10 $\mu g \cdot g^{-1}$ dry weight) to sediment-dwelling worms. All UV filters were detected in the worms after 28 days of exposure, but only BP3 was apparently bioaccumulated, with a biota sediment accumulation factor (BSAF) of 12.38 $\pm$ 4.65. However, metabolomic profiling revealed that OC was metabolized by the worms into 11 fatty acid conjugates, demonstrating that OC did also accumulate in the worms in the form of OC–fatty acid conjugates. Here, the sole quantification of the parent organic UV filter underestimated the accumulation factor and the exposure of organisms. In general, it is therefore important to pair the conventional method (BSAF calculus) with other techniques, such as metabolomics, to assess the actual potential for bioaccumulation of xenobiotics including transformed xenobiotics.

Keywords: *Hediste diversicolor*; bioaccumulation; UV filters; marine sediments; emerging pollutants

Citation: Clergeaud, F.; Fagervold, S.K.; Rodrigues, A.M.S.; Thorel, E.; Stien, D.; Lebaron, P. Transfer of 7 Organic UV Filters from Sediment to the Ragworm *Hediste diversicolor*: Bioaccumulation of Benzophenone-3 and Further Proof of Octocrylene Metabolism. *Pollutants* **2022**, *2*, 23–31. https://doi.org/10.3390/pollutants2010004

Academic Editor: Mauro Marini

Received: 13 November 2021
Accepted: 29 December 2021
Published: 4 February 2022

1. Introduction

Organic UV filters are commonly used in cosmetic products to protect skin against solar radiation (UV-A 320–400 nm and UV-B 280–320 nm). Although the presence of these compounds is essential for health reasons, their impact on marine ecosystems has recently become a concern due to potential toxic effects of certain filters and their bioaccumulative character [1,2]. Further, since organic UV filters are generally poorly soluble in water (logP > 3), they can accumulate in carbon-rich compartments, especially sediments [3,4]. For example, diethylhexyl butamido triazone (DBT), bis-ethylhexyloxyphenol methoxyphenyl triazine (BEMT), and methylene bis-benzotriazolyl tetramethylbutylphenol (MBBT) were found in the Villeneuve de la Raho Lake (France) sediments at 652.6, 115.0, and 75.2 $ng.g^{-1}$ dry weight, respectively [4]. These same UV filters are also found in the surface microlayer, with maximum concentrations of 43.3 ng/L for DBT, 5625.4 ng/L for BEMT, and 45.6 ng/L for MBBT. Meanwhile, these filters are poorly dispersed in the water column at maximum concentrations of 9.9 ng/L for DBT, 18.4 ng/L for BEMT, and below the detection limits for MBBT. Thus, organisms that spend at least a part of their life cycle in sediments could therefore be exposed to and potentially accumulate these UV filters,

increasing the risk for the transfer of these compound up the food chain. Indeed, organic UV filters have been detected in a wide diversity of marine animals such as bivalves [5,6], cephalopods [7,8], corals [9,10], fishes [8,11], mammals [12], and even bird eggs from a preserved area [13].

To fully assess the environmental risk of organic UV filters, it is necessary to study the transfer of these compounds from the sediment to sediment-dwelling organisms. *Hediste diversicolor*, the common ragworm, is a polychaete worm of the *Nereididae* family. It plays a key role in estuarine ecosystems, particularly for the biogeochemistry of sediments and element cycling [14]. Worms are highly exposed to sediment contaminants since they are burrowers and ingest large amounts of matter. They are prey for many marine animals (fish, birds, shrimp, crabs, etc.) and are an essential link in the food web [15]. Thus, sediment worms are among the basal links between sediment contamination and the bioaccumulation of contaminants up the food chain. Several studies have reported the accumulation of many toxic compounds, such as benzo[a]pyrene [16], silver nanoparticles [17], polychlorinated dibenzo-*p*-dioxins and dibenzofurans [18], metals, and PCBs [19], in *H. diversicolor*, but the bioaccumulation rate of many emerging contaminants including sunscreens have never been studied.

In this study, we assessed the transfer of seven common organic UV filters including benzophenone-3 (BP3), butyl methoxydibenzoylmethane (BM), 2-ethylhexyl salicylate (ES), octocrylene (OC), MBBT, DBT, and BEMT from sediment to worms. To accomplish this, concentrations of the UV filters in spiked sediments were measured and compared with the concentrations in worms after 28 days of exposure. The metabolome of the worms exposed to OC was also studied to examine the presence of any OC fatty acid conjugates.

2. Materials and Methods

2.1. Chemicals

The UV filters BP3, BEMT, BM, and MBBT were purchased from Sigma-Aldrich (Saint-Quentin Fallavier, France). ES, DBT, and OC were provided by Pierre Fabre Laboratories (Toulouse, France). The physicochemical properties of the UV filters used in this study are shown in Table 1. Analytical-grade dichloromethane (DCM), methanol (MeOH), formic acid (FA, 98%), vanillin (99%), sulfuric acid (97.5%), and phosphoric acid (85%) were obtained from Sigma-Aldrich. Pure water for chemical analysis was obtained from an Elga Purelab Flex System (Veolia LabWater STI, Antony, France). Glassware was cleaned and calcined at 400 °C for 2 h to remove all traces of organic matter.

Table 1. Structures and physicochemical properties of the seven UV filters.

Abbr. [a]	COSING Names (Alternative Names)	CAS Number	logP [b]	Formula	MW [c] (g.mol^{-1})
BEMT	bis-Ethylhexyloxyphenol methoxyphenyl triazine (Bemotrizinol)	187393-00-6	10.627	$C_{38}H_{49}N_3O_5$	627.8
BM	Butyl methoxydibenzoylmethane (Avobenzone)	70356-09-1	5.499	$C_{20}H_{22}O_3$	310.4
BP3	Benzophenone-3 (Oxybenzone)	131-57-7	3.514	$C_{14}H_{12}O_3$	228.8
DBT	Diethylhexyl butamido triazone (Iscotrizinol)	154702-15-5	12.004	$C_{44}H_{59}N_7O_5$	766.0
ES	2-Ethylhexyl salicylate (Octyl salicylate, Octisalate)	118-60-5	5.335	$C_{15}H_{22}O_3$	250.3
MBBT	Methylene bis-benzotriazolyl tetramethylbutylphenol (Bisoctrizole)	103597-45-1	15.451	$C_{41}H_{50}N_6O_2$	658.9
OC	Octocrylene	6197-30-4	7.083	$C_{24}H_{27}NO_2$	361.5

[a] abbreviation; [b] from Reaxys (https://www.reaxys.com/, accessed on 6 July 2021). For BM, the major tautomer (enol) logP is reported; [c] molecular weight.

2.2. Artificial Sediment Preparation and Spiking

Artificial sediment was produced, as already described [20] and was composed of sand with a particle size of 0.2–0.5 mm (sable de Loire SCALARE, Aquastore, France,

92.5 weight-%), kaolin clay (Merck, Darmstadt, Germany, 5 weight-%), and sphagnum blond peat (Florentaise, Saint-Mars-du-Désert, France, 2.5 weight-%). Homogenized sediments were spiked with a UV filter to a concentration of 10 $\mu g \cdot g^{-1}$ dry weight by adding 1 mg of UV filter diluted in DCM to 100 g dry sediment in a 600 mL beaker. The sediment was covered by DCM and was left to dry for at least 24 h while stirring the sediment to ensure that the compounds were homogeneously distributed.

2.3. Supply and Acclimatization of Worms

Hediste diversicolor specimens were ordered from Sustainable Feeds Ltd. (Brenkley Way, Seaton Burn, Newcastle upon Tyne, UK). The worms were sent overnight at 4 °C and were received approximately 24 h after shipment. The worms were transferred to 40 L glass tanks with artificial sediment and artificial seawater (Tropic Marin®, 34 $g \cdot L^{-1}$ in osmosis water). The tanks were equipped with an aeration pump and a ceramic bead filter enriched with microorganisms. The room temperature was kept at 16 °C, and the photoperiod was 16:8 h day/night at 250 lux. The worms were fed twice a week with seawater containing crushed TabiMin® (62.5 mg TabiMin® per 10 worms). All organisms were acclimated to these conditions for 2 weeks before they were used in exposure experiments.

2.4. Bioaccumulation Test in a Spiked Water–Sediment System

The exposure conditions and experimental setup were inspired by the OECD testing protocol for the "Sediment-Water *Lumbriculus* Toxicity Test Using Spiked Sediment" [21], and "Bioaccumulation in Sediment-dwelling Benthic Oligochaetes" [22]. Briefly, exposure tests were performed for 28 days in beakers each with 10 worms and in triplicate for each UV filter tested, in addition to negative controls.

Artificial seawater was added to 100 g of spiked sediment until the 400 mL mark in 600 mL beakers. This water level was kept constant throughout the incubation period and was oxygenated with an aeration pump and a plunging Pasteur pipette (2–4 bubbles per second). Water was added 24 h before the addition of worms to allow for equilibration of the UV filters between the sediment and the water. On the day of the start of the exposure (D0), the water was decanted off, and "day 0" sediment samples were collected in 3 different places in the beaker. The beaker was then filled with water again. The worms were allowed to depurate on wet tissue paper for approximately 3 h before the start of the test. Ten worms of similar sizes were added to each test beaker, and the worms were closely monitored for any avoidance behavior and to ensure that they were all burrowed within the first 24 h. The room temperature was kept at 16 °C, and the photoperiod was 16:8 h day/night at 250 lux. The water was changed (50%) twice a week. The water characteristics (NO_3, NO_2, NH_4, O_2, T, pH, and salinity) were closely monitored. The worms were fed twice a week with seawater containing crushed TabiMin® (62.5 mg for 10 worms).

At the end of the exposure (D28), the water was decanted off, and sediment samples were carefully collected at 6 different places in the beaker. The worms were then picked from each beaker and transferred on wet tissue paper to depurate for approximately 3 h. Then, the worms were counted and weighed before being transferred to a glass jar. They were then frozen at −80 °C and freeze-dried.

The potential transfer of UV filters from sediments to worms was estimated by assessing the Biota to Sediment Accumulation Factor (BSAF), which is defined by [22]:

$$\mathrm{BSAF} = \frac{\mathrm{Cw}/\mathrm{LP}}{\mathrm{Cs}/\mathrm{TOC}} \quad (1)$$

where Cw is the concentration of the UV filter in worms at day 28 ($\mu g \cdot g^{-1}$ dry weight of the whole body), which is then normalized by their lipid content (LP, in µg dw), and Cs is the concentration of the UV filter in sediment at day 28 ($\mu g \cdot g^{-1}$ dry weight), which is then normalized by the total organic carbon (TOC, in µg dw). We assumed that the TOC content of the sediment remained constant at 5%.

2.5. Extraction and Quantification of UV Filters

Sediment samples were frozen and lyophilized, followed by homogenization by grinding with a mortar and pestle. Sediment samples (200 mg) were extracted with DCM/MeOH 8:2 (1 mL) acidified with 0.1% FA. The suspensions were vortexed, subjected to ultrasound for 10 min, and centrifuged. The supernatant was collected, and the extraction was repeated. The mixed supernatants were dried in an HT-4X centrifugal vacuum evaporator. The residues were dissolved in acidified (0.1% FA) DCM/MeOH 8:2 (500 µL) for quantification of UV filters as described in [4], in which all analytical data including LODs and LOQs are reported.

Worms were also frozen and lyophilized, then inert sand was added to the dry worms. The mass of added sand was twice the dry weight of the pool of worms per condition. The mixture was homogenized using a mortar and pestle. A portion of the resulting powder (100 mg) was suspended in an acidified (0.1% FA) mixture of chloroform/methanol (2:1) in a glass tube. The slurry was vortexed and subjected to ultrasound for 20 min. The supernatant was transferred to a new tube, and the process was repeated once. A final centrifugation was performed to ensure that no solid material was suspended. The final supernatant was collected and dried in an HT-4X centrifugal vacuum evaporator (Genevac). Dried samples were dissolved in 500 µL of acidified (0.1% FA) DCM/MeOH (8:2) for injection (5 µL injected) into HPLC-UV for UV filter quantification. The UV filter concentrations were measured using an Ultimate 3000^{TM} HPLC system equipped with a diode array detector (Thermo Fisher Scientific) and a Phenomenex Kinetex Biphenyl 2.6 µm, 150 × 4.6 mm column, as described previously [4,23].

2.6. Lipid Quantification

The quantification of worm lipids was based on a sulfo-phospho-vanillic reaction, as already described [24]. The method was then adapted using a 96-well format [25] and involved generating and analyzing calibration standards (cholesterol in chloroform/MeOH (2:1)) each time a measurement was performed.

Worm powder was weighed in 3 different tubes (30 mg each, 2/3 inert sand and 1/3 ground lyophilized worms) and extracted as described above, except the solvents were not acidified. An amount of 100 µL of samples and standards was placed in a heating block set at 90 °C to allow the solvent to evaporate. Sulfuric acid (180 µL) was then added to each tube. After 10 min of incubation at 90 °C, the tubes were allowed to cool to room temperature before adding 500 µL of vanillin reagent (31 mg of vanillin, 12.5 mL of hot water, and 50 mL of 85% phosphoric acid) and vortexing. Finally, 200 µL from each tube was transferred into a 96-well plate. Lipid quantification was performed by measuring the absorbance at 530 nm on a Paradigm microplate reader (Beckman Coulter, Villepinte, France) [24].

$$Total\ lipids = (Abs_{530\,nm} \times Calibration) \times 0.8 \times \frac{15}{10} \quad (2)$$

The total lipid content can be calculated by converting the reading absorbance into a cholesterol concentration with the standard curve. Then, we applied a 0.8 coefficient (80 µg of cholesterol absorbed as 100 µg of total lipids) [24]. We multiplied by 15 to reach the total volume of the extract and divided by the 10 mg of dry worms we had from the start.

2.7. UHPLC-HRMS Profiling and Research of OC Metabolites

Ground lyophilized worm powder was extracted twice with 2 mL of DCM/MeOH 8:2, vortexed and ultrasonicated. The organic phases were gathered and dried. The 3 batches of worms exposed to OC were extracted in duplicate and analyzed. Chemical analyses were performed on samples diluted in DCM/MeOH 8:2, as already described for the coral *P. damicornis* [26]. Data were analyzed with Thermo Freestyle 1.6. OC-fatty acid conjugate sodium adducts collision-induced fragmentation yielded 2 typical products at m/z 272.0682 and 382.1778 (Figure 1). The corresponding ion chromatograms were extracted from the MS^2 trace. Where peaks were detected, the parent ion was designated as a putative OC

derivative and was annotated by examination of mass spectrometry data as reported by Stien et al. [26].

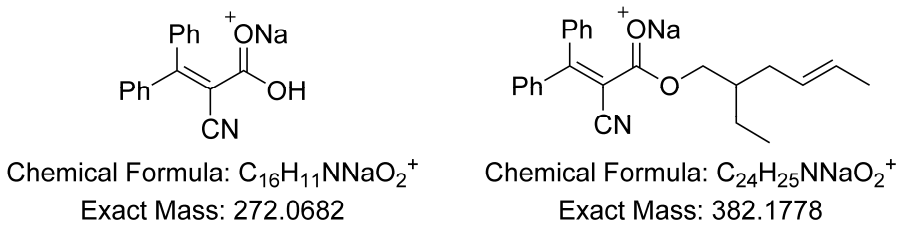

Figure 1. OC–fatty acid conjugates common products in collision-induced fragmentation of sodiated molecular ions.

2.8. Statistical Analyses

The *t* test was performed to compare the concentrations of UV filters in the sediments between days 0 and 28 using software R 4.0.3. The significance level was set at $p < 0.05$.

3. Results and Discussion

H. diversicolor was exposed to different UV filters for 28 days in a water sediment system. The worms did not show any avoidance behavior toward the spiked sediments, and all the worms had burrowed after 24 h of sediment contact. This suggests that all organisms were exposed to the contaminated sediment in the same way. Additionally, UV filters did not affect the survival of worms (data not shown). To assess the potential bioaccumulation of the UV filters, we measured the concentration of each of the UV filters in the sediment on day 0 and day 28, as well as the UV filter concentration in the exposed worms (Table 2). The lipid content of each batch of worms was also measured.

Table 2. Concentration of UV filters found in sediments at day 0 and day 28 ($\mu g \cdot g^{-1}$ dry weight), lipid content in worms at day 28 (µg dry weight), concentrations of UV filters in *Hediste diversicolor* at the end of the 28-day exposure ($\mu g \cdot g^{-1}$ dry weight), and Biota-Sediment Accumulation Factor (BSAF) calculated for each UV filter. The percentage of total organic carbon (% TOC) used for calculation of BSAF was 5%.

	C_{sed}/D0 [a]	C_{sed}/D28 [a]	Lipid Cont. [b]	C_{worms}/d28 [c]	BSAF
BEMT	6.7 ± 1.1	6.7 ± 1.3	130.9 ± 11.2	2.5 ± 0.8	0.2 ± 0.0
BM	2.9 ± 0.5	2.9 ± 0.7	81.8 ± 8.9	0.4 ± 0.1	0.1 ± 0.0
BP3	5.0 ± 1.2	2.5 ± 0.5	62.7 ± 8.6	33.9 ± 10.0	12.4 ± 4.6
DBT	7.0 ± 3.3	6.4 ± 1.4	104.7 ± 8.8	4.5 ± 0.8	0.3 ± 0.0
ES	4.0 ± 1.8	3.6 ± 2.2	88.4 ± 3.8	1.6 ± 0.3	0.3 ± 0.1
MBBT	6.4 ± 1.6	5.5 ± 2.9	75.7 ± 1.8	1.3 ± 1.1	0.1 ± 0.0
OC	6.1 ± 1.6	7.2 ± 1.0	64.7 ± 3.5	2.2 ± 0.3	0.2 ± 0.0

[a] Concentration in sediment at day 0 and day 28, expressed in $\mu g \cdot g^{-1}$ dw; [b] Lipid content in worms at day 28, expressed in µg dw; [c] Concentration in worms at day 28, expressed in $\mu g \cdot g^{-1}$ dw.

For six UV filters, there was no significant difference between the sediment concentrations at D0 and D28 (*t*-test, $p > 0.05$) (Table 2). For BP3, we observed a 24.7 ± 6.5% loss from D0 to D28 (*t*-test, $p = 5.27 \times 10^{-4}$). One reason might be the higher water solubility of BP3. Further, BP3 accumulated in the worms, a phenomenon that could also be responsible for the lower sediment concentration at D28 (Table 2).

Table 2 shows UV filter concentrations in the worms after 28 days of exposure. Concentrations ranged from 0.43 ± 0.07 $\mu g \cdot g^{-1}$ dw for BM to 33.90 ± 10.09 $\mu g \cdot g^{-1}$ dw for BP3. All UV filters were able to migrate from the sediment to the biotic compartment, but except for BP3, we observed no bioaccumulation of the UV filters after 28 days of exposure (BSAF < 1). The BSAF for BP3 was 12.38 ± 4.65. This is in line with Blüthgen et al. [27], in which the BP3 bioconcentration factor in zebrafish was between 19 and 94.

Additionally, a potential transfer of BP3 in the food web with a trophic magnification factor of 1.23 was also demonstrated in the literature [28]. Since marine worms are prey for many marine animals, these results show that BP3 may represent a risk for the health of aquatic ecosystems. Indeed, BP3 was shown to disrupt the endocrine system by inducing estrogenic activity in an in vitro gene assay of zebrafish [29] and to induce a vitellogenin protein in male Japanese rice fish [30]. BP3 can also cause developmental neurotoxicity in zebrafish [31]. The genotoxic potential of this UV filter was also demonstrated in the coral *Stylophora pistillata* [32].

Based on this standard protocol for measuring BSAF, OC does not appear to bioaccumulate. However, in previous work in which we measured the effect of OC on the coral *Pocillopora damicornis*, we demonstrated that OC was transformed in the coral and concluded that measuring the concentration of unmodified OC was not sufficient to assess its actual BSAF [26]. Since similar OC derivatives have been detected in human urine [33,34], there are questions as to whether this process of oxidation and esterification of OC in animals might be widespread and may thus result in the global underestimation of OC contamination and rising bioaccumulation. Therefore, the extracts of the OC-exposed worms were analyzed by LC-MS/MS to search for possible OC derivatives. We were able to annotate 11 OC-fatty acid conjugates in the worms exposed to OC (Figure 2, Table 3). Six of the OC metabolites were identical to those already described from the metabolome of *Pocillopora damicornis* coral exposed to OC [26]. Another five compounds bearing somewhat more saturated fatty acids than those with the same chain lengths from the coral were new (C18:0, C20:1, C20:2, C22:2). Compounds **1**–**11** analytical data are provided in the Supporting Materials. Clearly, as for the coral, these compounds were biosynthesized by the worms by oxidation of the ethylhexyl side chain and subsequent esterification of the hydroxyl group with fatty acids originating from the pool of fatty acids available in the worms. This result is all the more disturbing because in the case of this marine worm, the OC derivatives peak integrations were between 50 and 1800 times larger than the untransformed OC peak integration. Similarly, we have previously found peaks up to 100 times higher than OC chromatographic peak integration in corals and concluded that the actual OC accumulation rate in the ocean food chain should be re-evaluated and that future titrations should include OC fatty acid conjugates [26]. *H. diversicolor* is known to be an active metabolizer of organic contaminants such as benzo[a]pyrene, as reported by Driscoll and McElroy [16]. This may explain why the OC derivatives were detected in such a high proportion in worm tissues. The sum of OC derivative relative integrations is 5869, indicating that the quantification of OC alone may underestimate the overall OC derivative concentration by a factor of several thousand while when calculated with OC alone, the BSAF was 0.23 (Table 2). Hence, it is reasonable to conclude that OC actually bioaccumulates in worms in the form of OC–fatty acid conjugates.

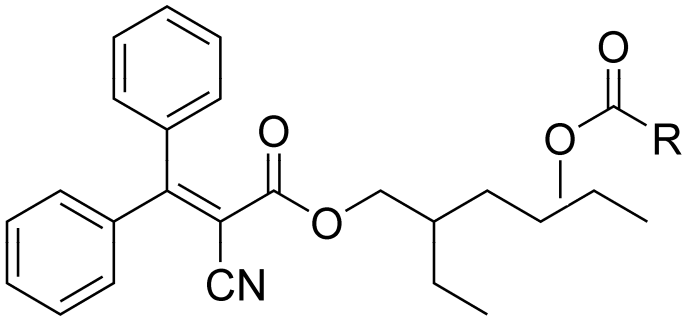

Figure 2. General structure of OC–fatty acid conjugates. The substitution site is undetermined, and the R group is a saturated or unsaturated linear alkyl chain (see Table 3).

Table 3. OC–fatty acid conjugates annotated in *H. diversicolor* worms exposed to OC.

Cmpd. #	$-O_2CR$	t_R (min)	Exp. m/z [a]	Rel. Area [b]
1	C16:0	15.44	638.4177	543
2	C18:0	16.46	666.4500	553
3	C18:1	15.52	664.4338	713
4	C18:1	15.67	664.4330	384
5	C20:1	16.51	692.4647	1767
6	C20:2	15.67	690.4496	676
7	C20:2	15.77	690.4495	749
8	C20:3	14.99	688.4339	120
9	C20:5	13.71	684.4025	47
10	C22:2	16.63	718.4806	263
11	C22:6	14.05	710.4181	54

[a] $[M+Na]^+$ ion; [b] Average peak area relative to average OC peak area, on 3 replicates. Cmpd.# compounds numbers.

4. Conclusions

We show that all seven UV filters tested in this study can disperse in a complex medium and migrate to the biotic compartment. However, only BP3 was demonstrated to bioaccumulate (BSAF > 1). The use of this UV filter represents a potential risk to marine ecosystems because BP3 might be biomagnified and exert many direct and indirect toxic effects through the food web.

Although parent OC did not appear to accumulate in worms (BSAF < 1), we detected 11 more lipophilic metabolites in the fatty tissues of the exposed worms. The very high relative integration of OC derivative peaks suggests that OC might in fact accumulate and that the total OC derivative BSAF might be very high. Our results further demonstrate that the study of any parent organic UV filters alone may largely underestimate the exposure of organisms to xenobiotics and that xenobiotic metabolites should be annotated and included in the measurement of BSAF to better assess the risk for bioaccumulation of xenobiotics in living beings.

Supplementary Materials: The following are available online at https://www.mdpi.com/article/10.3390/pollutants2010004/s1. Figure S1. Extracted ion chromatograms for compounds 1 to 11 ($[M+Na]^+$) in the profile of worms Hediste diversicolor exposed to OC.; Figure S2. MS spectrum of compound 1; Figure S3. Expanded MS spectrum of compound 1; Figure S4. MS/MS spectrum of ion at m/z 638.4180 $[(1+Na)^+]$; Figure S5. MS spectrum of compound 2; Figure S6. Expanded MS spectrum of compound 2; Figure S7. MS/MS spectrum of ion at m/z 666.4498 $[(2+Na)^+]$; Figure S8. MS spectrum of compound 3; Figure S9. Expanded MS spectrum of compound 3; Figure S10. MS/MS spectrum of ion at m/z 664.4336 $[(3+Na)^+]$ et $[(4+Na)^+]$; Figure S11. MS spectrum of compound 4; Figure S12. Expanded MS spectrum of compound 4; Figure S13. MS spectrum of compound 5; Figure S14. Expanded MS spectrum of compound 5; Figure S15. MS/MS spectrum of ion at m/z 692.4654 $[(5+Na)^+]$; Figure S16. MS/MS spectrum of ion at m/z 687.5099 $[(5+NH_4)^+]$; Figure S17. MS spectrum of compound 6; Figure S18. Expanded MS spectrum of compound 6; Figure S19. MS/MS spectrum of ion at m/z 690.4498 $[(6+Na)^+]$; Figure S20. MS spectrum of compound 7; Figure S21. Expanded MS spectrum of compound 7; Figure S22. MS spectrum of compound 8; Figure S23. Expanded MS spectrum of compound 8; Figure S24. MS/MS spectrum of ion at m/z 688.4336 $[(8+Na)^+]$; Figure S25. MS spectrum of compound 9; Figure S26. Expanded MS spectrum of compound 9; Figure S27. MS/MS spectrum of ion at m/z 684.4023 $[(9+Na)^+]$; Figure S28. MS spectrum of compound 10; Figure S29. Expanded MS spectrum of compound 10; Figure S30. MS/MS spectrum of ion at m/z 718.4811 $[(10+Na)^+]$; Figure S31. MS spectrum of compound 11; Figure S32. Expanded MS spectrum of compound 11. Table S1. List of OC metabolites.

Author Contributions: Conceptualization, P.L.; data curation, E.T., S.K.F., F.C. and D.S.; formal analysis, D.S. and A.M.S.R.; funding acquisition, P.L.; project administration, P.L.; investigation, F.C., S.K.F. and E.T.; methodology, F.C., S.K.F. and E.T.; Roles/writing-original draft, F.C.; writing-review & editing, D.S. and P.L. All authors have read and agreed to the published version of the manuscript.

Funding: The work reported in this article was financed in the context of the Pierre Fabre Skin Protect Ocean Respect action (Grant Number 2018-02108). It was neither supervised nor audited by Pierre Fabre Laboratories. The interpretation and views expressed in this manuscript are not those of the company.

Institutional Review Board Statement: Not applicable.

Informed Consent Statement: Not applicable.

Data Availability Statement: The analytical and spectral data of OC metabolites presented in this study are available in Supporting Information.

Acknowledgments: We thank the BIO2MAR platform from the Observatoire Océanologique de Banyuls-sur-Mer for providing technical support and access to instrumentation.

Conflicts of Interest: The authors declare no conflict of interest.

References

1. Lozano, C.; Givens, J.; Stien, D.; Matallana-Surget, S.; Lebaron, P. Bioaccumulation and toxicological effects of UV-filters on marine species. In *Sunscreens in Coastal Ecosystems: Occurrence, Behavior, Effect and Risk*; The Handbook of Environmental Chemistry; Springer: Berlin/Heidelberg, Germany, 2020; Volume 94, pp. 85–130.
2. Huang, Y.; Law, J.C.; Lam, T.K.; Leung, K.S. Risks of organic UV filters: A review of environmental and human health concern studies. *Sci. Total Environ.* **2021**, *755*, 142486. [CrossRef]
3. Ramos, S.; Homem, V.; Alves, A.; Santos, L. Advances in analytical methods and occurrence of organic UV-filters in the environment—A review. *Sci. Total Environ.* **2015**, *526*, 278–311. [CrossRef]
4. Fagervold, S.K.; Rodrigues, A.M.S.; Rohée, C.; Roe, C.; Bourrain, M.; Stien, D.; Lebaron, P. Occurrence and environmental distribution of 5 UV filters during the summer season in different water bodies. *Water Air Soil Pollut.* **2019**, *230*, 172. [CrossRef]
5. Sang, Z.; Leung, K.S.-Y. Environmental occurrence and ecological risk assessment of organic UV filters in marine organisms from Hong-Kong coastal waters. *Sci. Total Environ.* **2016**, *566*, 489–498. [CrossRef] [PubMed]
6. He, K.; Hain, E.; Timm, A.; Tarnowski, M.; Blaney, L. Occurrence of antibiotics, estrogenic hormones, and UV-filters in water, sediment, and oyster tissue from the Chesapeake Bay. *Sci. Total Environ.* **2019**, *650*, 3101–3109. [CrossRef] [PubMed]
7. Peng, X.; Fan, Y.; Jin, J.; Xiong, S.; Liu, J.; Tang, C. Bioaccumulation and biomagnification of ultraviolet absorbents in marine wildlife of the Pearl River Estuarine, South China Sea. *Environ. Pollut.* **2017**, *225*, 55–65. [CrossRef]
8. Cunha, S.C.; Trabalón, L.; Jacobs, S.; Castro, M.; Fernandez-Tejedor, M.; Granby, K.; Verbeke, W.; Kwadijk, C.; Ferrari, F.; Robbens, J.; et al. UV-filters and musk fragrances in seafood commercialized in Europe Union: Occurrence, risk and exposure assessment. *Environ. Res.* **2018**, *161*, 399–408. [CrossRef]
9. Tsui, M.M.P.; Lam, J.C.W.; Ng, T.Y.; Ang, P.O.; Murphy, M.B.; Lam, P.K.S. Occurrence, distribution, and fate of organic UV filters in coral communities. *Environ. Sci. Technol.* **2017**, *5*, 4182–4190. [CrossRef]
10. Mitchelmore, C.L.; He, K.; Gonsior, M.; Hain, E.; Heyes, A.; Clark, C.; Younger, R.; Schmitt-Kopplin, P.; Feerick, A.; Conway, A.; et al. Occurrence and distribution of UV-filters and other anthropogenic contaminants in coastal surface water, sediment, and coral tissue from Hawaii. *Sci. Total Environ.* **2019**, *670*, 398–410. [CrossRef]
11. Langford, K.H.; Reid, M.J.; Fjeld, E.; Øxnevad, S.; Thomas, K.V. Environmental occurrence and risk of organic UV filters and stabilizers in multiple matrices in Norway. *Environ. Int.* **2015**, *80*, 1–7. [CrossRef]
12. Gago-Ferrero, P.; Alonso, M.B.; Bertozzi, C.P.; Marigo, J.; Barbosa, L.; Cremer, M.; Secchi, E.R.; Domit, C.; Azevedo, A.; Lailson-Brito, J., Jr.; et al. First Determination of UV Filters in Marine Mammals. Octocrylene Levels in Franciscana Dolphins. *Environ. Sci. Technol.* **2013**, *47*, 5619–5625. [CrossRef] [PubMed]
13. Molins-Delgado, D.; Máñez, M.; Andreu, A.; Hiraldo, F.; Eljarrat, E.; Barceló, D.; Díaz-Cruz, M.S. A Potential New Threat to Wild Life: Presence of UV Filters in Bird Eggs from a Preserved Area. *Environ. Sci. Technol.* **2017**, *51*, 10983–10990. [CrossRef] [PubMed]
14. Davey, J.T. The architecture of the burrow of *Nereis diversicolor* and its quantification in relation to sediment-water exchange. *J. Exp. Mar. Biol. Ecol.* **1994**, *179*, 115–129. [CrossRef]
15. Scaps, P. A review of the biology, ecology and potential use of the common ragworm *Hediste diversicolor* (O. F. Müller) (Annelida: Polychaeta). *Hydrobiologia* **2002**, *470*, 203–218. [CrossRef]
16. Driscoll, S.K.; McElroy, A.E. Bioaccumulation and metabolism of benzo(a)pyrene in three species of polychaete worms. *Environ. Toxicol. Chem.* **1996**, *15*, 1401–1410. [CrossRef]
17. Cong, Y.; Banta, G.T.; Selck, H.; Berhanu, D.; Valsami-Jones, E.; Forbes, V.E. Toxicity and bioaccumulation of sediment-associated silver nanoparticles in the estuarine polychaete, *Nereis (Hediste) diversicolor*. *Aquat. Toxicol.* **2014**, *156*, 106–115. [CrossRef]
18. Picone, M.; Delaney, E.; Tagliapietra, D.; Guarneri, I.; Ghirardini, A.V. Bioaccumulation of polychlorinated dibenzo-p-Dioxins (PCDDs) and dibenzofurans (PVDFs) in *Hediste diversicolor* (polychaeta: Nereididae). *Front. Ecol. Evol.* **2020**, *8*, 235. [CrossRef]
19. Ruus, A.; Schaanning, M.; Øxnevad, S.; Hylland, K. Experimental results on bioaccumulation of metals and organic contaminants from marine sediments. *Aquat. Toxicol.* **2005**, *72*, 273–292. [CrossRef]

20. Le Bihanic, F.; Perrichon, P.; Landi, L.; Clérandeau, C.; Le Menach, K.; Budzinski, H.; Cousin, X.; Cachot, J. Development of a reference artificial sediment for chemical testing adapted to the MELA sediment contact assay. *Environ. Sci. Pollut.* **2014**, *21*, 13689–13702. [CrossRef]
21. *Test No. 225: Sediment-Water Lumbriculus Toxicity Test Using Spiked Sediment*; OECD Guidelines for the Testing of Chemicals, Section 2; Éditions OCDE: Paris, France, 2007.
22. *Test No. 315: Bioaccumulation in Sediment-Dwelling Benthic Oligochaetes*; OECD Guidelines for the Testing of Chemicals, Section 3; Éditions OCDE: Paris, France, 2008.
23. Rodrigues, A.M.S.; Lebaron, P.; Downs, C.A.; Stien, D. Optimization method for titrating sunscreen organic ultraviolet filters in coastal sands. *J. Sep. Sci.* **2021**, *44*, 3338–3347. [CrossRef]
24. Barnes, H.; Blackstock, J. Estimation of lipids in marine animals and tissues: Detailed investigation of the sulphophosphovanillin method for 'total' lipids. *J. Exp. Mar. Biol. Ecol.* **1973**, *12*, 103–118. [CrossRef]
25. Inouye, L.S.; Lotufo, G.R. Comparison of macro-gravimetric and micro-colorimetric lipid determination methods. *Talanta* **2006**, *70*, 584–587. [CrossRef]
26. Stien, D.; Clergeaud, F.; Rodrigues, A.M.S.; Lebaron, K.; Pillot, R.; Romans, P.; Fagervold, S.; Lebaron, P. Metabolomics reveal that octocrylene accumulates in *Pocillopora damicornis* tissues as fatty acid conjugates and triggers coral cell mitochondrial dysfunction. *Anal. Chem.* **2019**, *91*, 990–995. [CrossRef] [PubMed]
27. Blüthgen, N.; Zucchi, S.; Fent, K. Effects of the UV-filter benzophenone-3 (oxybenzone) at low concentrations in zebrafish (*Danio rerio*). *Toxicol. Appl. Pharmacol.* **2012**, *263*, 184–194. [CrossRef]
28. Yang, H.; Lu, G.; Yan, Z.; Liu, J.; Dong, H.; Bao, X.; Zhang, X.; Sun, Y. Residues, bioaccumulation, and trophic transfer of pharmaceuticals and personal care products in highly urbanized rivers affected by water diversion. *J. Hazard. Mater.* **2020**, *391*, 122245. [CrossRef]
29. Schreurs, R.; Lanser, P.; Seinen, W.; van der Burg, B. Estrogenic activity of UV-filters determined by an in vitro reporter gene assay and an in vivo transgenic Zebrafish assay. *Arch. Toxicol.* **2002**, *76*, 257–261. [CrossRef]
30. Schneider, S.L.; Lim, H.W. Review of environmental effects of oxybenzone and other sunscreen active ingredients. *J. Am. Acad. Dermatol.* **2019**, *80*, 266–271. [CrossRef]
31. Tao, J.; Bai, C.; Chen, Y.; Zhou, H.; Liu, Y.; Shi, Q.; Pan, W.; Dong, H.; Li, L.; Xu, H.; et al. Environmental relevant concentrations of benzophenone-3 induced developmental neurotoxicity in zebrafish. *Sci. Total Environ.* **2020**, *721*, 137686. [CrossRef]
32. Downs, C.A.; Kramarsky-Winter, E.; Segal, R.; Fauth, J.; Knutson, S.; Bronstein, O.; Ciner, F.R.; Jeger, R.; Lichtenfeld, Y.; Woodley, C.M.; et al. Toxicopathological effects of the sunscreen UV filter, oxybenzone (benzophenone-3), on coral planulae and cultured primary cells and its environmental contamination in Hawaii and the U.S. Virgin Islands. *Arch. Environ. Contam.* **2016**, *70*, 265–288. [CrossRef]
33. Bury, D.; Belov, V.; Yulin, Q.; Hayen, H.; Volmer, D.A.; Brüning, T.; Koch, H.M. Determination of urinary metabolites of the emerging UV filter octocrylene by online-SPE-LC-MS/MS. *Anal. Chem.* **2018**, *90*, 944–951. [CrossRef] [PubMed]
34. Bury, D.; Modick-Biermann, H.; Leibold, E.; Brüning, T.; Koch, H.M. Urinary metabolites of the UV filter octocrylene in humans as biomarkers of exposure. *Arch. Toxicol.* **2019**, *93*, 1227–1238. [CrossRef] [PubMed]